NASA/TM-97-206218

Stress Analysis of B-52 Pylon Hooks for Carrying the X-38 Drop Test Vehicle

William L. Ko
Dryden Flight Research Center
Edwards, California

The NASA STI Program Office . . . in Profile

Since its founding, NASA has been dedicated to the advancement of aeronautics and space science. The NASA Scientific and Technical Information (STI) Program Office plays a key part in helping NASA maintain this important role.

The NASA STI Program Office is operated by Langley Research Center, the lead center for NASA's scientific and technical information. The NASA STI Program Office provides access to the NASA STI Database, the largest collection of aeronautical and space science STI in the world. The Program Office is also NASA's institutional mechanism for disseminating the results of its research and development activities. These results are published by NASA in the NASA STI Report Series, which includes the following report types:

- TECHNICAL PUBLICATION. Reports of completed research or a major significant phase of research that present the results of NASA programs and include extensive data or theoretical analysis. Includes compilations of significant scientific and technical data and information deemed to be of continuing reference value. NASA's counterpart of peer-reviewed formal professional papers but has less stringent limitations on manuscript length and extent of graphic presentations.

- TECHNICAL MEMORANDUM. Scientific and technical findings that are preliminary or of specialized interest, e.g., quick release reports, working papers, and bibliographies that contain minimal annotation. Does not contain extensive analysis.

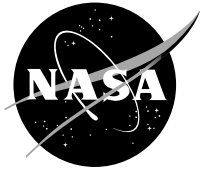- CONTRACTOR REPORT. Scientific and technical findings by NASA-sponsored contractors and grantees.

- CONFERENCE PUBLICATION. Collected papers from scientific and technical conferences, symposia, seminars, or other meetings sponsored or cosponsored by NASA.

- SPECIAL PUBLICATION. Scientific, technical, or historical information from NASA programs, projects, and mission, often concerned with subjects having substantial public interest.

- TECHNICAL TRANSLATION. English-language translations of foreign scientific and technical material pertinent to NASA's mission.

Specialized services that complement the STI Program Office's diverse offerings include creating custom thesauri, building customized databases, organizing and publishing research results . . . even providing videos.

For more information about the NASA STI Program Office, see the following:

- Access the NASA STI Program Home Page at *http://www.sti.nasa.gov*

- E-mail your question via the Internet to help@sti.nasa.gov

- Fax your question to the NASA Access Help Desk at (301) 621-0134

- Telephone the NASA Access Help Desk at (301) 621-0390

- Write to:
  NASA Access Help Desk
  NASA Center for AeroSpace Information
  800 Elkridge Landing Road
  Linthicum Heights, MD 21090-2934

NASA/TM-97-206218

Stress Analysis of B-52 Pylon Hooks for Carrying the X-38 Drop Test Vehicle

William L. Ko
Dryden Flight Research Center
Edwards, California

October 1997

Available from:

CONTENTS

ABSTRACT

The finite-element structural analysis method was used in a two-dimensional stress concentration analysis of a new pylon hook for carrying the X-38 lifting body atmospheric drop test vehicle on the B-52 carrier aircraft. The stress distributions in the hook were obtained, and the critical stress points were identified. The functional relationships between the applied hook load and the induced maximum tangential and shear stresses were established for setting the limit hook load for test flights. By properly representing the X-38 hook with an equivalent curved beam, the conventional curved beam theory predicted the values of the maximum tangential and shear stresses quite close to those calculated from the finite-element analysis. The equivalent curved beam method may be of practical value during the initial stage of the hook design in estimating the critical stresses and failure loads with reasonable accuracy.

NOMENCLATURE

a	radius of hook inner circular boundary region, in.
b	radius of hook outer circular boundary region, in.
c	inner to outer radii ratio, $c = a/b$
CRV	crew return vehicle
DAST	drone for aerodynamic and structural testing
E	Young's modulus, lb/in^2
g	curved beam depth parameter for end moment loading
g_1	curved beam depth parameter for end force loading
h	thickness of hook, in.
JLOC	joint location
l	moment arm of hook load, in.
M	end moment for equivalent curved beam, $M = Pl$, in-lb
P	hook load or end force for equivalent curved beam, lb
P_{FE}	partial hook load for finite-element model, $P_{FE} = 0.01(P/h)$, lb
P_f^s	ultimate hook load in shear failure, lb
P_f^t	ultimate hook load in tensile failure, lb
q	distributed hook load, lb/in.
q_{FE}	nodal force for finite-element model, $\Sigma q_{FE} = P_{FE}$, lb/node

r	radial distance, in.
r_s	radial location of maximum shear stress $\tau_{r\theta}\big|_{max}$, in.
x,y	rectangular Cartesian coordinates
θ	angular coordinate measured from horizontal x-axis, deg
θ_c	angular location of critical stress point for $\sigma_t\big|_{max}$, deg
ν	Poisson's ratio
σ_f	tensile failure stress, lb/in^2
σ_r	total radial stress in the curved beam, lb/in^2
σ_r^M	radial stress in the curved beam due to end moment M, lb/in^2
σ_r^P	radial stress in the curved beam due to end force P, lb/in^2
σ_t	tangential stress in the hook from finite-element analysis, lb/in^2
σ_θ	total tangential stress in the curved beam, lb/in^2
σ_θ^M	tangential stress in the curved beam due to end moment M, lb/in^2
σ_θ^P	tangential stress in the curved beam due to end force P, lb/in^2
$\sigma_\theta\big|_{\theta\,=\,29.25^\circ}$	value of σ_θ at $\theta = 29.25^\circ$, lb/in^2
$\sigma_\theta\big|_{\theta\,=\,\theta_c}$	value of σ_θ at $\theta = \theta_c$, lb/in^2
τ_f	shear failure stress, lb/in^2
$\tau_{r\theta}$	total shear stress in the curved beam, lb/in^2
$\tau_{r\theta}^M$	shear stress in the curved beam due to end moment M, lb/in^2
$\tau_{r\theta}^P$	shear stress in the curved beam due to end force P, lb/in^2
τ_{xy}	shear stress in the hook from finite-element analysis, lb/in^2
$(\,)\big|_{max}$	maximum value of $(\,)$

INTRODUCTION

The vehicle designated the X-38 is a lifting body flight vehicle that will develop the technologies for the emergency crew return vehicle (CRV) for the International Space Station. The operational CRV will be 28.5 ft long and 14.5 ft wide. The structure will be aluminum with a shell of graphite-cyanate ester

epoxy. The thermal protection system will consist of improved Space Shuttle Orbiter-derived blankets and tiles. The vehicle will have four control surfaces: two body flaps for pitch and roll control, and two rudders for yaw and roll control. The operational CRV will reenter from orbit and glide unpowered like the Space Shuttle Orbiter, but unlike the Orbiter, it will not employ a steep high-energy approach landing. Because of potentially excessive landing speeds for the small but heavy vehicle, the CRV will use a steerable ram-air parachute below Mach 0.25 and flare to a soft landing. The entire sequence from reentry to landing is to be fully autonomous without any need for human intervention.

The experimental X-38 vehicle shown in figure 1 is a nearly full-scale vehicle and is 24.5 ft long and 11.5 ft wide, weighing 16,557 lb. The X-38 will be carried under the wing of the NASA Dryden B-52 aircraft on two new L-shaped hooks on a specially designed pylon up to an altitude of 40,000 ft to conduct nonpiloted, free-flight drop tests. The main purposes of the tests are to evaluate touchdown dynamics of the vehicle-parachute combination, to study free-flight vehicle stability and control characteristics in transonic and subsonic flight, to assess parachute system reliability, and to demonstrate free-flight vehicle energy management and positioning capabilities.

The L-shaped hooks will induce stress concentration in the inner circular boundary region and, therefore, the new hook must be designed in such a way as to reduce the stress concentration and eliminate fatigue concerns during the X-38 program. Thus, an examination of the induced stress field in the new hook is important to validate its structural integrity.

This report concerns the finite-element stress analysis of a newly designed hook for carrying the X-38 vehicle and documents the analyses performed. The report presents the analytical stress distributions in the new hook to locate the critical stress points in tension and shear. Certain functional relationships between the hook load and the induced maximum tangential stress and the maximum shear stress are established, and an equivalent curved beam theory is developed to analyze the hook.

X-38 HOOK DESCRIPTIONS

Figure 2 shows a sketch of the B-52 carrying the X-38 vehicle on new identical front and rear hooks (called X-38 hooks) on a dedicated pylon. The X-38 vehicle rolling motion during captive-carry flight is restrained by two sway braces as shown in the figure. Figure 3 shows the geometry of the L-shaped X-38 hook. The X-38 hook is made of 4340 steel that was heat-treated and has the following material properties

$$E = 29 \times 10^6 \text{ lb/in}^2$$

$$\nu = 0.32$$

$$\sigma_f = 101,000 \text{ lb/in}^2$$

$$\tau_f = 60,600 \text{ lb/in}^2$$

The hook has thickness $h = 2.8$ in. The inner circular arc boundary of the hook has a radius of 0.5 in., and the outer circular arc boundary has a radius of 2 in. The centers of the two radii do not coincide. Because of the nonconcentric nature of the inner and outer circular arc boundaries, the hook is clearly not a conventional curved beam.

The X-38 design hook load, *P*, is 42,027 lb. This hook load consists of four components:

- Static load due to X-38 weight
- Static load due to tightening of sway braces
- Aerodynamic load generated from aerodynamic force exerted on X-38 during captive flight
- Inertia load arising from X-38 vertical inertia load (2.2 times gravitational acceleration) during captive flight

The hook load *P* is located at a distance $l = 0.75$ in. from the *y*-axis (fig. 3). To avoid local point loading, the hook load is distributed over the flat horizontal surface of the hook through a rounded triangular sleeve that can rotate freely around a circular pin (fig. 3) when the hooks swing to launch the X-38 vehicle.

FINITE-ELEMENT ANALYSIS

The Structures Performance and Resizing (SPAR) finite-element computer program (ref. 1) was used in the stress concentration analysis of the X-38 hooks.

Finite-Element Modeling

Because the critical stress points are in the lower L-shaped region of the hook, only this region was modeled. Figure 4 shows the finite-element model generated for the X-38 hook. The model has 1212 joint locations (JLOC) and consists of 40 triangular combined membrane and bending elements (E33 elements) and 1125 quadrilateral combined membrane and bending elements (E43 elements). To maintain proper element length to thickness ratios of the two-dimensional elements (E33, E43) for computational accuracy, the thickness of the model was chosen to be 0.01 in.; namely, the model is actually a thin slice cut out from the full thickness of the hook.

Constraints

The upper left corner point is fixed, and the upper horizontal straight boundary is allowed to move freely in the horizontal direction (*x*-direction) with the vertical motion (*y*-direction) constrained.

Loadings

Two hook-loading conditions were considered: a concentrated load or a distributed load (fig. 4). The purpose of these dual analyses is to compare the stress concentrations under different loading conditions. The loads shown in figure 4 are the actual hook loads and not the partial loads for input to the finite-element model. For the 0.01-in. thick finite-element model, the applied partial hook load P_{FE} was calculated from

$$P_{FE} = \frac{P}{h} \times 0.01 = \frac{42,027}{2.8} \times 0.01 = 150.10 \text{ lb} \tag{1}$$

For the concentrated load case, because there is no node coincidental to the actual loading point, the applied load P_{FE} was divided into two parts and applied at two adjacent nodes between which the actual loading point lies, preserving the effective loading point location of $l = 0.74375$ in.

4

For the distributed load case, the applied load P_{FE} is equally distributed over the nodes lying in the hook flat horizontal boundary, and the load intensity q_{FE} is applied at each node where $\Sigma q_{FE} = P_{FE}$. The span of this distributed loading zone is the length of one flat side of the rounded triangular sleeve (fig. 3), again preserving the effective loading point location.

EQUIVALENT CURVED BEAM ANALYSIS

The shape of the inner rounded boundary of the hook is a circular arc (fig 3). However, the corresponding outer curved boundary is a nonconcentric circular arc (i.e., the inner and outer circular arcs have different centers). The hook curved region, therefore, is clearly not of a conventional curved beam geometry. The purpose of this section is to represent the hook with an equivalent curved beam, and to explore whether the curved beam theory might roughly estimate the critical stress values. As will be seen later, this simple approach turned out to be of great practical value in estimating the critical stress values and the hook failure loads by using a desk calculator (or a simple Fortran program) before conducting the time-consuming finite-element stress analysis.

Curved Beam Geometry

For analysis, the curved region of the hook is represented by an equivalent curved beam of one quadrant ($0 < \theta < \pi/2$; fig. 5). The inner radius, a, of the equivalent curved beam has an identical radius as that of the hook ($a = 0.5$ in.). The outer radius, b, of the equivalent curved beam was so chosen that its circular boundary will circumscribe the outer boundary of the hook, which resulted in a radius $b = 4.28$ in.

The equivalent loading condition on the curved beam may be considered as the summation of two loading cases: bending under the end force P and bending under the end moment $M = Pl$ (refs. 2–4; fig. 5).

Stress Equations

The induced bending stresses for end force loading (ref. 5) can be expressed as

$$\sigma_r^P(r, \theta) = \frac{P}{bhg_1}\left[\frac{r}{b} + c^2\left(\frac{b}{r}\right)^3 - \left(1 + c^2\right)\frac{b}{r}\right]\sin\left(\frac{\pi}{2} - \theta\right) \tag{2}$$

$$\sigma_\theta^P(r, \theta) = \frac{P}{bhg_1}\left[3\frac{r}{b} - c^2\left(\frac{b}{r}\right)^3 - \left(1 + c^2\right)\frac{b}{r}\right]\sin\left(\frac{\pi}{2} - \theta\right) \tag{3}$$

$$\tau_{r\theta}^P(r, \theta) = -\frac{P}{bhg_1}\left[\frac{r}{b} + c^2\left(\frac{b}{r}\right)^3 - \left(1 + c^2\right)\frac{b}{r}\right]\cos\left(\frac{\pi}{2} - \theta\right) \tag{4}$$

where c is the radii ratio of a/b, and g_1 is defined as

$$g_1 = 1 - c^2 + \left(1 + c^2\right)\ln(c) \tag{5}$$

For end moment loading, the induced bending stresses can be expressed as

$$\sigma_r^M(r) = -\frac{M}{b^2 hg}\left\{c^2\ln(c)\left[1 - \left(\frac{b}{r}\right)^2\right] - \left(1 - c^2\right)\ln\left(\frac{b}{r}\right)\right\} \tag{6}$$

$$\sigma_\theta^M(r) = -\frac{M}{b^2 hg}\left\{1 - c^2 + c^2\ln(c)\left[1 + \left(\frac{b}{r}\right)^2\right] - \left(1 - c^2\right)\ln\left(\frac{b}{r}\right)\right\} \tag{7}$$

$$\tau_{r\theta}^M = 0 \tag{8}$$

where g is defined as

$$g = \left(\frac{1 - c^2}{2}\right)^2 - c^2\left[\ln(c)\right]^2 \tag{9}$$

The total stresses in the equivalent curved beam are then obtained by the summation of the above two similar stress components.

$$\sigma_r = \sigma_r^P + \sigma_r^M \tag{10}$$

$$\sigma_\theta = \sigma_\theta^P + \sigma_\theta^M \tag{11}$$

$$\tau_{r\theta} = \tau_{r\theta}^P + \tau_{r\theta}^M \tag{12}$$

The maximum tangential stress $\sigma_\theta|_{max}$ is located at point ($r = a$, $\theta = 0°$), but the maximum shear stress $\tau_{r\theta}|_{max}$ is located at another point ($r = r_s$, $\theta = 90°$) where r_s is given by

$$r_s = \frac{1}{\sqrt{2}}\left[\sqrt{\left(a^2 + b^2\right)^2 + 12a^2 b^2} - \left(a^2 + b^2\right)\right]^{1/2} \tag{13}$$

Equation (13) was obtained by differentiating equation (4) with respect to r and then setting the resultant equation equal to zero. Notice that r_s is also the radial location of the maximum radial stress $\sigma_r^P|_{max}$ (tangential location is $\theta = 0°$) induced by force P (eq. (2)). Fortran programs for calculating the distributions of σ_θ and $\tau_{r\theta}$ in the equivalent curved beam are attached in appendix A.

RESULTS

The following sections present the results of both the finite-element analysis and the equivalent curved beam analysis.

6

Finite-Element Analysis

The deformations, stress distributions, and load-stress equations for the X-38 hook are presented in the following.

Stresses and Deformations

Figures 6 and 7, respectively, show the deformed shapes of the X-38 hook under concentrated and distributed loadings. The vertical deflections at the horizontal tip of the hook are 4.04×10^{-3} in. and 4.11×10^{-3} in., respectively, for the two loading cases. Notice that these deflections are close to each other.

Figures 8 and 9 show the distributions of tangential stress σ_t along the inner boundary of the hook for the concentrated load and distributed load cases, respectively. For the concentrated load case (fig. 8), the element with the maximum tangential stress $\sigma_t|_{max} = 53,510$ lb/in^2 is at the inner boundary with angular location $\theta = \theta_c = 24.75°$. For the distributed load case (fig. 9), the element with maximum tangential stress $\sigma_t|_{max} = 53,964$ lb/in^2 is at the inner boundary with angular location $\theta = \theta_c = 29.25°$.

For the above L-shaped X-38 hook, just as for other B-52 hooks analyzed in the past (figs. B-1 through B-8 in appendix B; ref. 6), the critical stress points are not located exactly at $\theta_c = 0°$ as in the case of the classical curved beam (eq. (3)), but are located within the region $11.25° < \theta_c < 36.25°$.

Figures 10 and 11 show the distributions of tangential stress σ_t and shear stress τ_{xy} along the critical hook cross-section lines for the concentrated and distributed loading cases, respectively. For both of the loading cases, the τ_{xy} distributions profiles are saddle shaped with the $\tau_{xy}|_{max}$ points located relatively near the upper hook boundary. For the concentrated load case (fig. 10), the maximum shear stress $\tau_{xy}|_{max} = 11,004$ lb/in^2 lies in the vertical cross-section slightly to the right of the loading point. The maximum shear stress $\tau_{xy}|_{max} = 9,093$ lb/in^2 for the distributed load case (fig. 11) lies in the vertical cross-section passing through the right-hand termination point of the distributed loading zone. Table 1 compares the angular locations of the critical tangential stress points and the maximum stresses induced in the X-38 hook under concentrated and distributed loadings calculated from finite-element analysis.

Table 1. Comparison of finite-element results of concentrated and distributed loadings of the X-38 hook.

Loading case	θ_c, deg	$\sigma_t|_{max}$, lb/in^2	$\tau_{xy}|_{max}$, lb/in^2
Concentrated load	24.75	53,510	11,004
Distributed load	29.25	53,964	9,093

The results of the distributed load case (actual loading situation, fig. 3) in table 1 will be compared with the results using the equivalent curved beam theory.

Load-Stress Equations

From the results of the stress analysis (figs. 8–11), the functional relationships between the hook load P and the maximum stresses may be established as follows:

Concentrated load:

$$\frac{\sigma_t|_{max}}{P} = 1.2732 \text{ lb/in}^2/\text{lb} \tag{14}$$

$$\frac{\tau_{xy}|_{max}}{P} = 0.2618 \text{ lb/in}^2/\text{lb} \tag{15}$$

Distributed load:

$$\frac{\sigma_t|_{max}}{P} = 1.2840 \text{ lb/in}^2/\text{lb} \tag{16}$$

$$\frac{\tau_{xy}|_{max}}{P} = 0.2164 \text{ lb/in}^2/\text{lb} \tag{17}$$

If $\sigma_t|_{max}$ and $\tau_{xy}|_{max}$ in equations (14) through (17) reach their respective failure stress levels ($\sigma_t|_{max} = \sigma_f$ and $\tau_{xy}|_{max} = \tau_f$), the load-stress equations (14) through (17) can then be used to calculate the hook failure loads in tension and in shear as

Concentrated load:

$$P^t_f = 0.7854 \ \sigma_f \text{ lb} \tag{18}$$

$$P^s_f = 3.8192 \ \tau_f \text{ lb} \tag{19}$$

Distributed load:

$$P^t_f = 0.7788 \ \sigma_f \text{ lb} \tag{20}$$

$$P^s_f = 4.6219 \ \tau_f \text{ lb} \tag{21}$$

Using the failure stress values of the hook material given earlier ($\sigma_f = 101,000 \text{ lb/in}^2$ and $\tau_f = 60,600 \text{ lb/in}^2$), the hook failure loads in tension and in shear may be calculated from equations (14) through (17). Table 2 shows the results.

Table 2. Failure hook loads in tension and shear ($\sigma_f = 101{,}000$ lb/in^2, $\tau_f = 60{,}600$ lb/in^2).

Loading case	P_f^t, lb	P_f^s, lb
Concentrated load	79,325	231,444
Distributed load	78,659	280,087

Table 2 shows that the X-38 hook will definitely fail in tension rather than in shear. The limit hook load for test flights may then be established by applying a proper safety factor.

Equivalent Curved Beam Analysis

The results of the stress analysis of the equivalent curved beam and the established functional relationships between the hook load and the critical stresses are presented in the following sections.

Stress Distributions

Figure 12 shows the distribution of the total tangential stress along the inner boundary of the equivalent curved beam, induced by the combined loading of the end force P (where $P = 42{,}027$ lb) and the end moment M (where $M = Pl = 42{,}027 \times 0.74375 = 31{,}258$ in-lb). The magnitudes of the bending stress components (σ_θ^P and σ_θ^M) are indicated in the figure for comparison. At $\theta = 29.25°$, which is the location of $\sigma_t|_{max}$ point in the X-38 hook for the distributed load case, σ_θ has the value of $\sigma_\theta|_{\theta = 29.25°} = 54{,}636$ lb/in^2. This value is close to the values of $\sigma_t|_{max} = 53{,}964$ lb/in^2 calculated from the finite-element analysis of the actual hook (fig. 9). This discovery is significant and of great practical value because with only hand calculations using the curved beam stress equations, one can quickly estimate the intensity of the critical stress in the L-shaped X-38 hook during the initial design phase before initiating the time-consuming finite-element analysis.

Figure 13 shows the distributions of σ_θ and $\tau_{r\theta}$ along their respective critical cross-section lines. The maximum shear stress $\tau_{r\theta}|_{max} = 9{,}327$ lb/in^2 lies in the $\theta = 90°$ plane and is located at a radial distance of $r_s = 0.8441$ in. (0.3441 in. from the hook horizontal boundary). This value is also close to $\tau_{xy}|_{max} = 9{,}093$ lb/in^2 calculated from the finite-element analysis (fig. 11). Table 3 summarizes these results.

Table 3. Comparison of critical stresses in X-38 hook calculated from the finite-element analysis and the equivalent curved beam theory.

Mode of analysis	$\sigma_t|_{max}$, lb/in^2	$\tau_{xy}|_{max}$, lb/in^2
Finite-element analysis	53,964	9,093
Equivalent curved beam theory	54,636	9,327
Percent error	1.25	2.57

Notice that the errors are amazingly low. This finding implies the powerful practical value of the equivalent curved beam theory.

Load-Stress Equations

From figure 13, the relationships between the hook load P and the tangential stress σ_θ at $\theta = 29.25°$ and the maximum shear stress are $\tau_{r\theta}|_{max}$ established as follows:

$$\frac{\sigma_\theta|_{\theta = 29.25°}}{P} = 1.3000 \text{ lb/in}^2/\text{lb} \tag{22}$$

$$\frac{\tau_{r\theta}|_{max}}{P} = 0.2219 \text{ lb/in}^2/\text{lb} \tag{23}$$

Substitution of $(\sigma_\theta|_{\theta = 29.25°}$ and $\tau_{r\theta}|_{max})$ in equations (22) and (23), respectively, with their failure stresses $(\sigma_f$ and $\tau_f)$ yields the following hook failure loads in tension and in shear.

$$P_f^t = 0.7692 \ \sigma_f \ \text{lb} \tag{24}$$

$$P_f^s = 4.5065 \ \tau_f \ \text{lb} \tag{25}$$

Applying the given values of $(\sigma_f = 101,000 \text{ lb/in}^2$ and $\tau_f = 60,600 \text{ lb/in}^2)$, the failure load equations (24) and (25) become

$$P_f^t = 77,689 \text{ lb} \tag{26}$$

$$P_f^s = 273,096 \text{ lb} \tag{27}$$

Notice that the levels of the hook failure loads are close to those shown in table 2, indicating the great practical value of using the equivalent curved beam theory in the initial stage of hook design for quick estimation of the hook failure loads.

Practical Approach

The practical way to use the equivalent curved beam theory may be summarized as follows. During the early stage of hook design, for a trial hook geometry and the loading condition, an equivalent curved beam of one quadrant may be created. The inner circular boundary of the equivalent curved beam should match the inner circular boundary of the hook. The outer circular boundary of the equivalent curved beam should circumscribe the outermost curved boundary of the hook. The curved beam theory is then used to calculate stress distributions in the equivalent curved beam. The maximum shear stress lies in the $\theta = 90°$ plane and at a known radial distance r_s given by equation (13). However, the angular location θ_c (which is configuration dependent) of the critical tangential stress point in the hook is still unknown. A reasonable guess is to use $\theta_c = 26°$, the average value of the known θ_c of past B-52 hooks (appendix B) and of the X-38 hook, to obtain the critical tangential stress at $r = a$. Through this approach, the approximate hook failure loads in tension and shear may be estimated.

In addition to the X-38 hook case, the validity of the equivalent curved beam theory was further tested for the previous B-52 hooks shown in appendix B (ref. 6). The tangential stresses σ_θ at the already known θ_c locations, and at the averaged angular location $\theta_c = 26°$, were calculated. The results are compared with the finite-element solutions and are shown in table 4.

The relatively low solution errors indicate the powerful practical value of the equivalent curved beam theory in estimating the critical stress levels during the preliminary hook design.

Table 4. Comparison of critical tangential stresses in B-52 hooks calculated from the finite-element and the equivalent curved beam analyses.

Hook / Item	X-38 hook	Front hook	Old rear hook	DAST rear hook	New rear hook
θ_c, deg	29.25	26.25	36.25	11.25	28.75
$\sigma_t|_{max}$, lb/in^2	53,964	73,522	172,200	100,700	100,400
$\sigma_\theta|_{\theta=\theta_c}$, lb/in^2	54,636	64,088	165,567	96,557	94,138
Percent error	+1.25	−12.83	−3.85	−4.11	−6.24
Averaged θ_c, deg	26	26	26	26	26
$\sigma_\theta|_{\theta=26°}$, lb/in^2	55,945	64,212	179,721	89,550	95,992
Percent error	+3.67	−12.66	+4.37	−11.07	−4.39

CONCLUDING REMARKS

Finite-element stress concentration analysis was performed on the X-38 hook subjected to concentrated and distributed loadings. The locations and the magnitudes of the tensile and shear critical stresses were identified. The key findings are as follows:

1. The X-38 hook was found to fail in tension rather than in shear.

2. The critical tensile stress point is located on the X-38 hook inner boundary at $\theta = 24.75°$ and $\theta = 29.25°$, respectively, for the concentrated and distributed loadings, where θ is an angle measured from the horizontal x-axis.

3. The maximum shear stress point is located in the cross-section near the root of the X-38 hook horizontal arm and is relatively closer to the upper horizontal boundary.

4. By representing the X-38 and other B-52 hooks with equivalent curved beams, the classical curved beam theory could be used to quickly estimate the critical stresses in the hooks and the hook failure loads with reasonable accuracy, before performing the more detailed finite-element analysis.

Dryden Flight Research Center
National Aeronautics and Space Administration
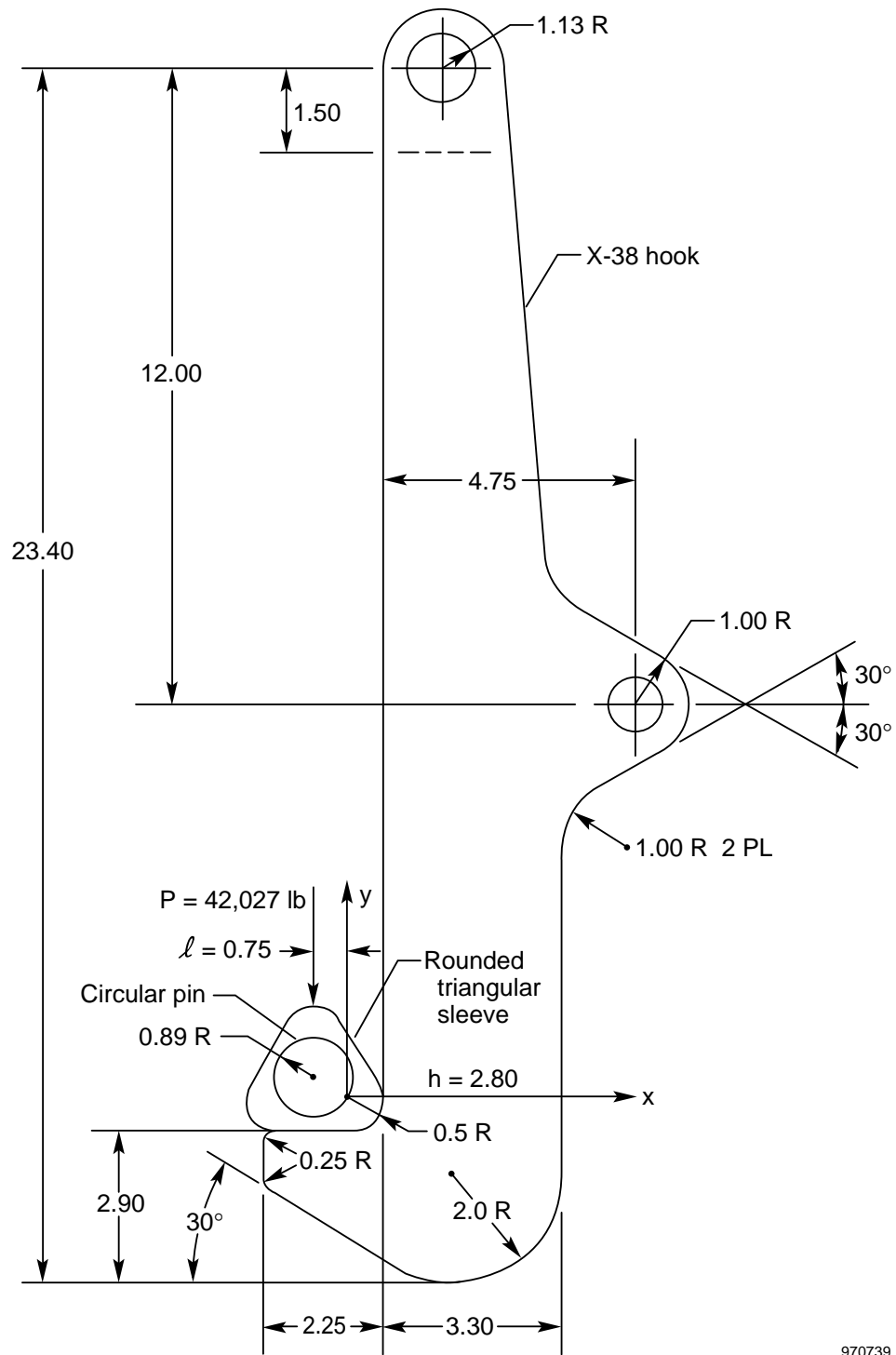*Edwards, California, April 11, 1997*

EC96 43737-13

Figure 1. The X-38 lifting body atmospheric test vehicle to be launched from the B-52 aircraft.
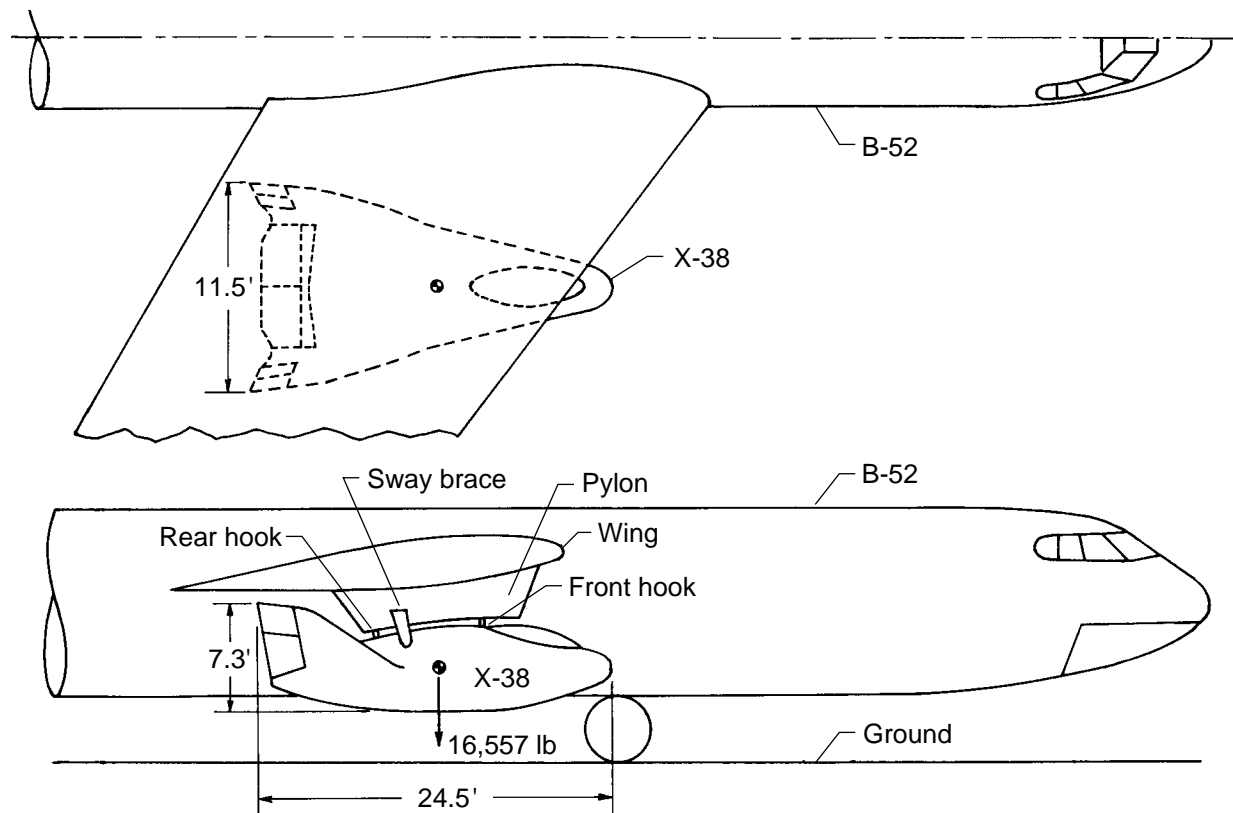
970738

Figure 2. Sideview of the X-38 lifting body atmospheric test vehicle mated to the B-52 pylon through two new hooks.

Figure 3. Geometry of the X-38 hook for carrying X-38 atmospheric test vehicle; dimensions in inches, except as noted.
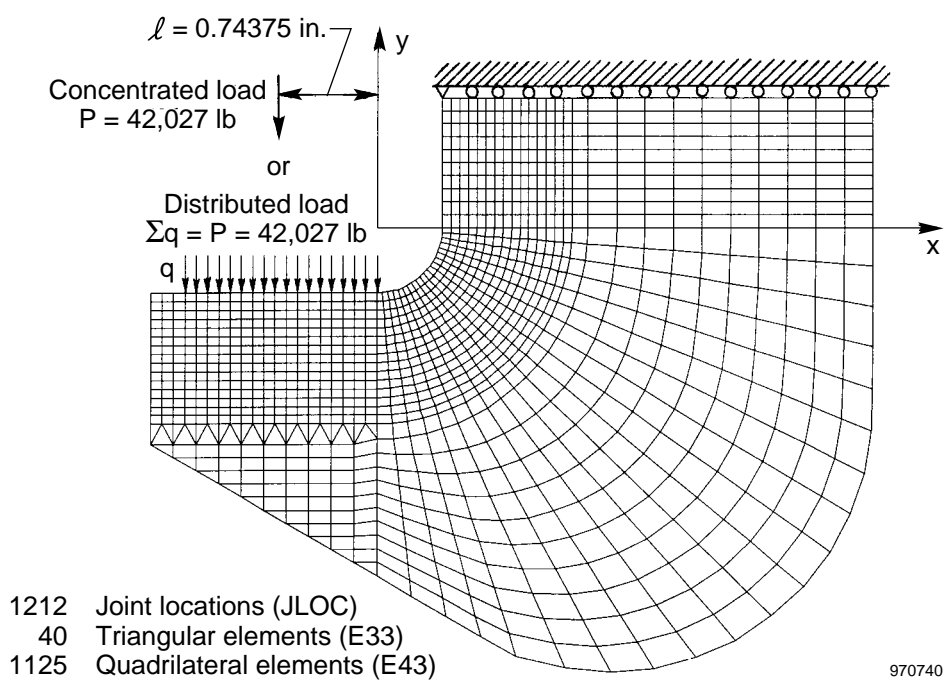
$\ell = 0.74375$ in.

y

Concentrated load
P = 42,027 lb

or

Distributed load
$\Sigma q = P = 42,027$ lb

x

q

1212   Joint locations (JLOC)
  40   Triangular elements (E33)
1125   Quadrilateral elements (E43)

970740

Figure 4. SPAR finite-element model for the X-38 hook.

14

Actual case

P ℓ

X-38 hook

Bending under
end force

P

a

θ

b

a = 0.5 in.
b = 4.28 in.
ℓ = 0.74375 in.

Equivalent
curved beam

Bending under
end moment

ℓ

P

P

M = Pℓ

a

θ

b

a = 0.5 in.
b = 4.28 in.
ℓ = 0.74375 in.

Equivalent
curved beam

970741
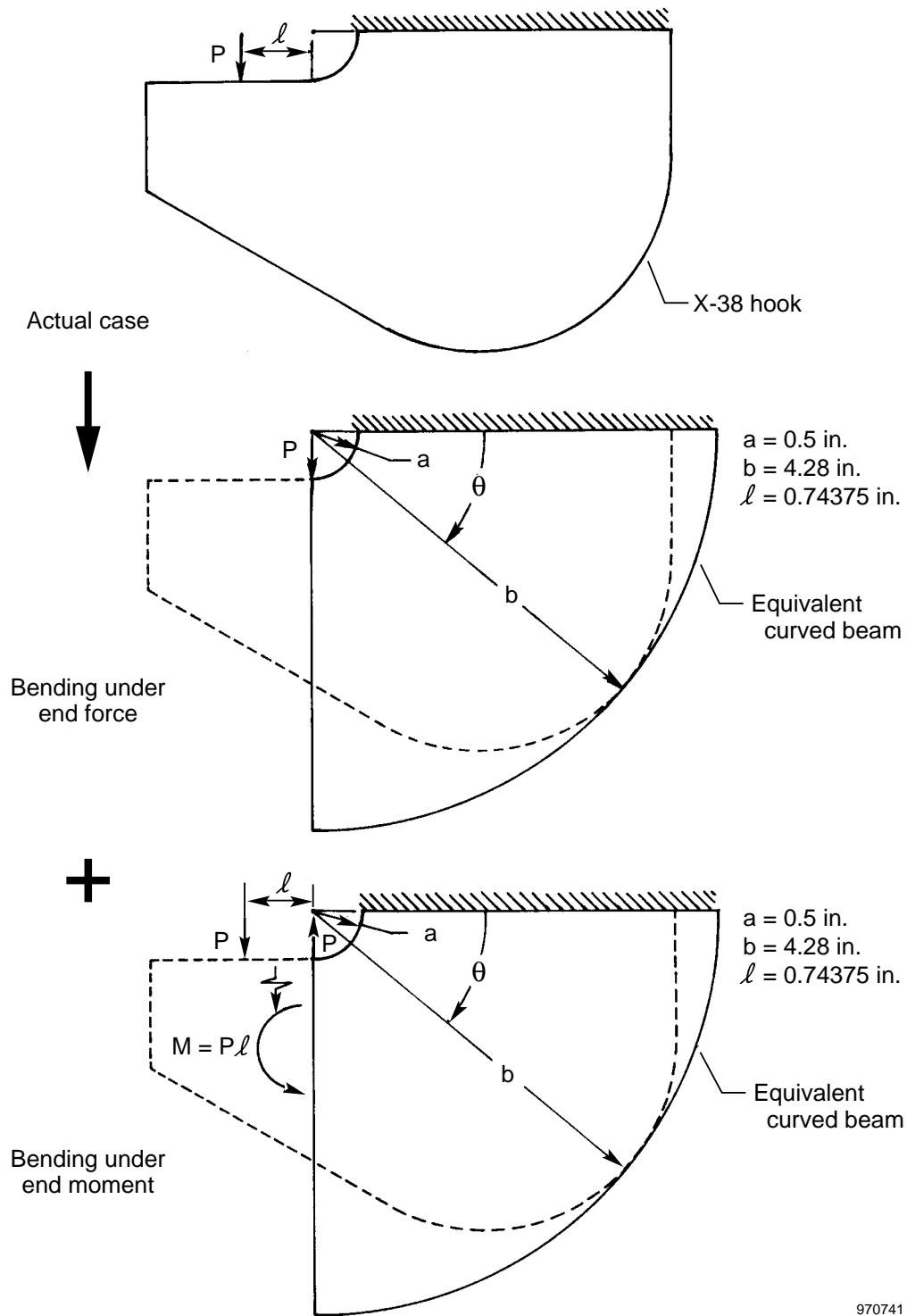
Figure 5. Representation of the X-38 hook geometry with an equivalent curved beam.
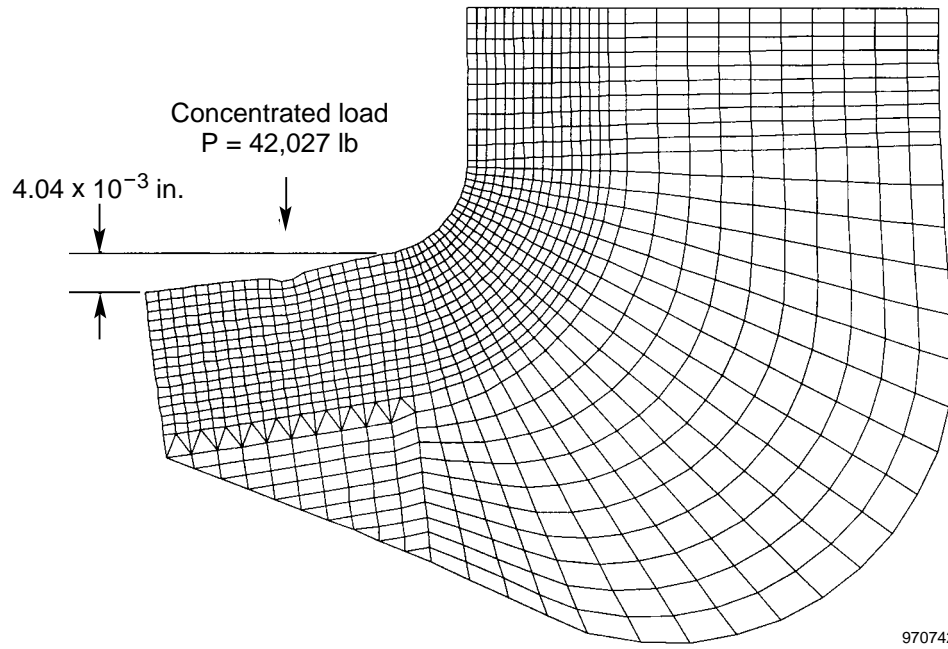
Figure 6. Deformed shape of the X-38 hook under concentrated load; $P = 42{,}027$ lb.
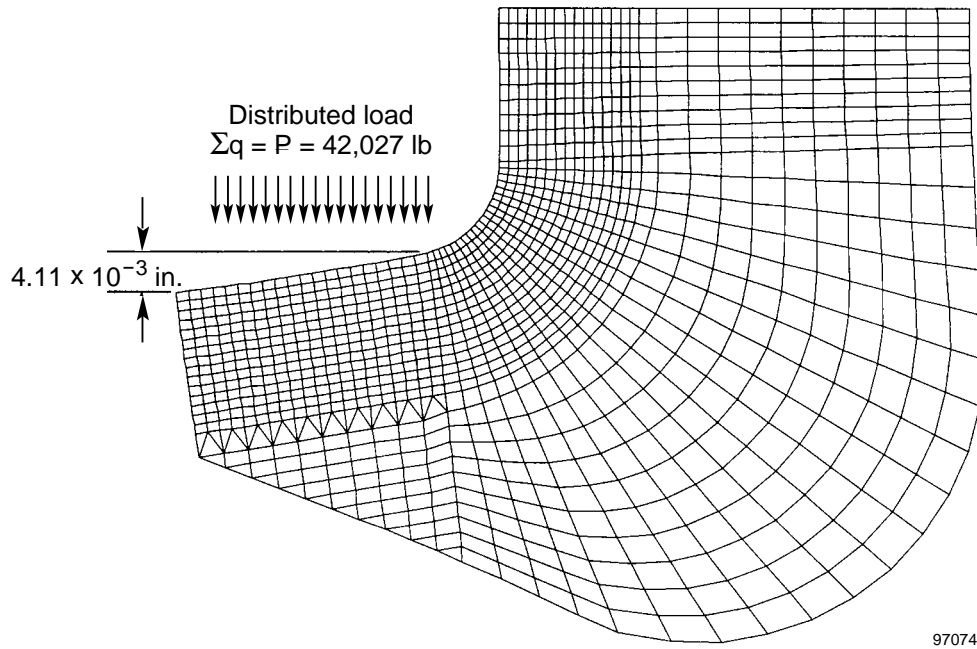
Figure 7. Deformed shape of the X-38 hook under distributed load; $\Sigma q = P = 42{,}027$ lb.
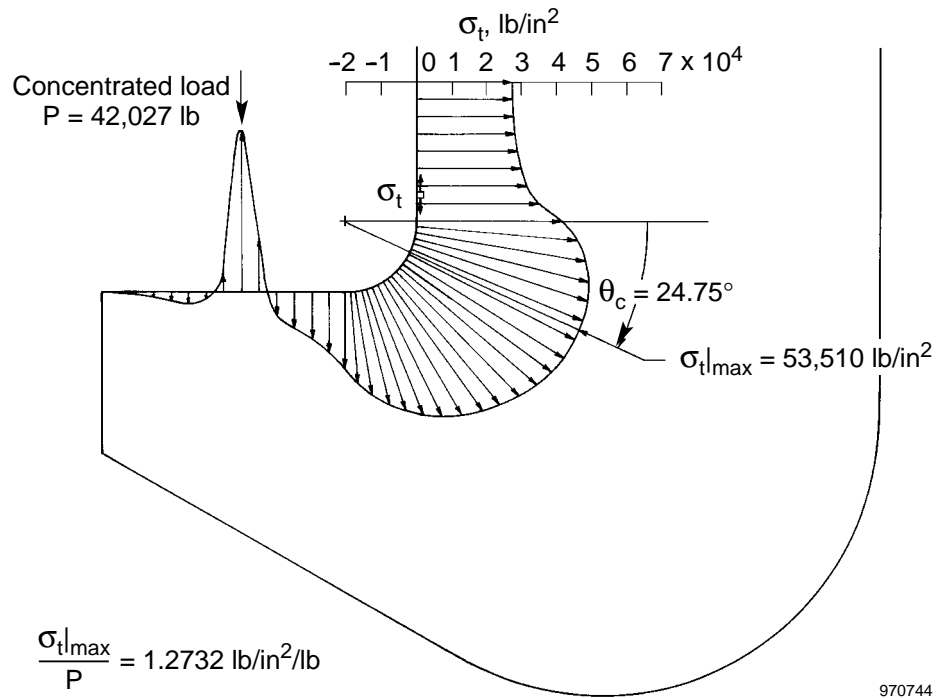
Figure 8. Distribution of tangential stress σ_t along inner boundary of the X-38 hook; concentrated load $P = 42{,}027$ lb.
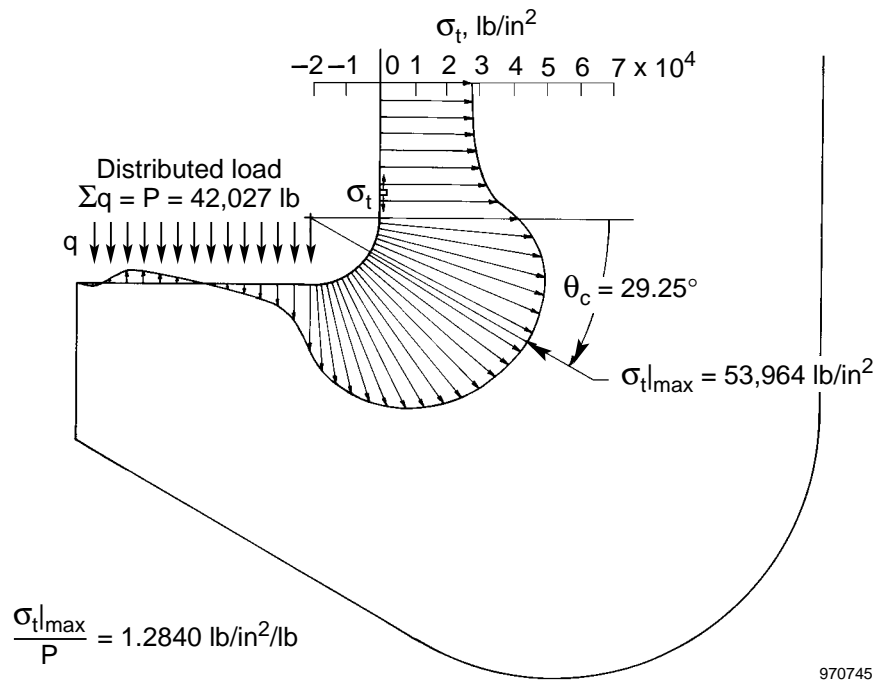
Figure 9. Distribution of tangential stress σ_t along inner boundary of the X-38 hook; distributed load $\Sigma q = P = 42{,}027$ lb.
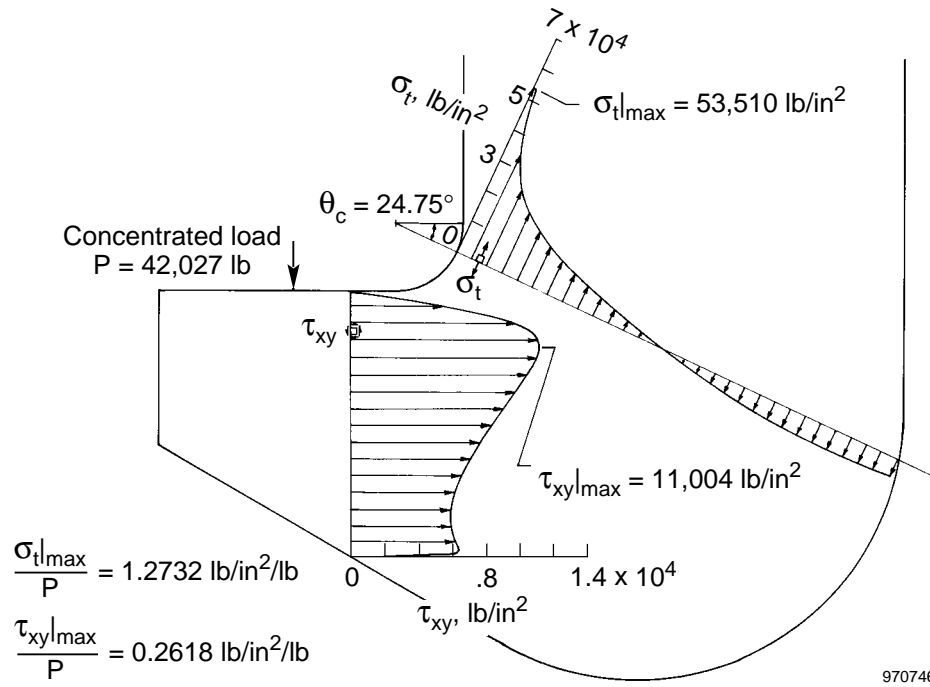
Figure 10. Distributions of tangential stress σ_t and shear stress τ_{xy} along their respective critical cross section lines; concentrated load $P = 42{,}027$ lb.
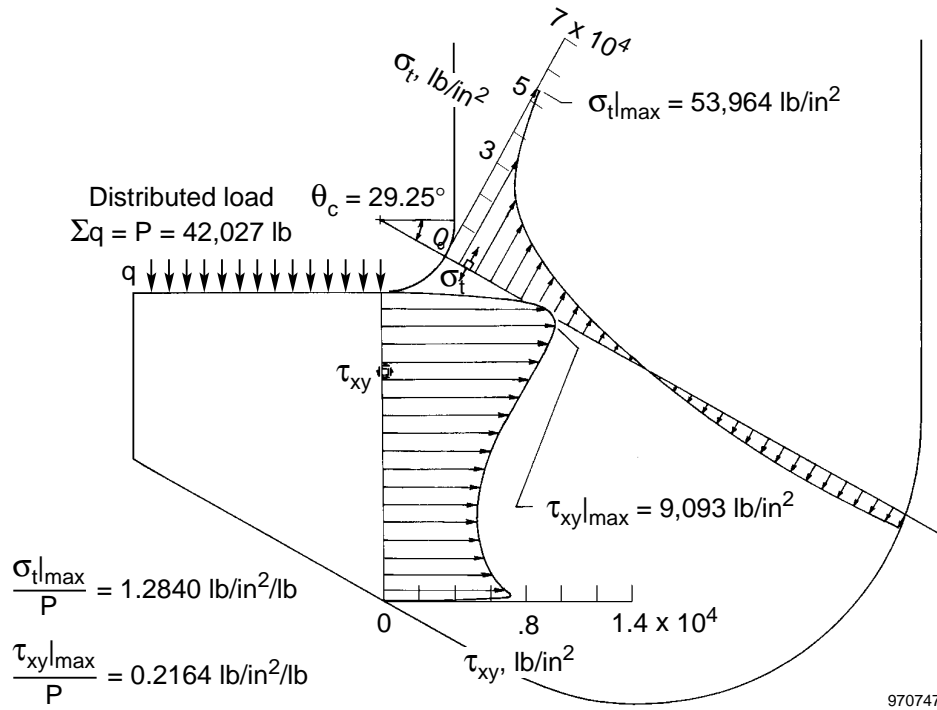
Figure 11. Distributions of tangential stress σ_t and shear stress τ_{xy} along their respective critical cross section lines; distributed load $\Sigma q = P = 42{,}027$ lb.
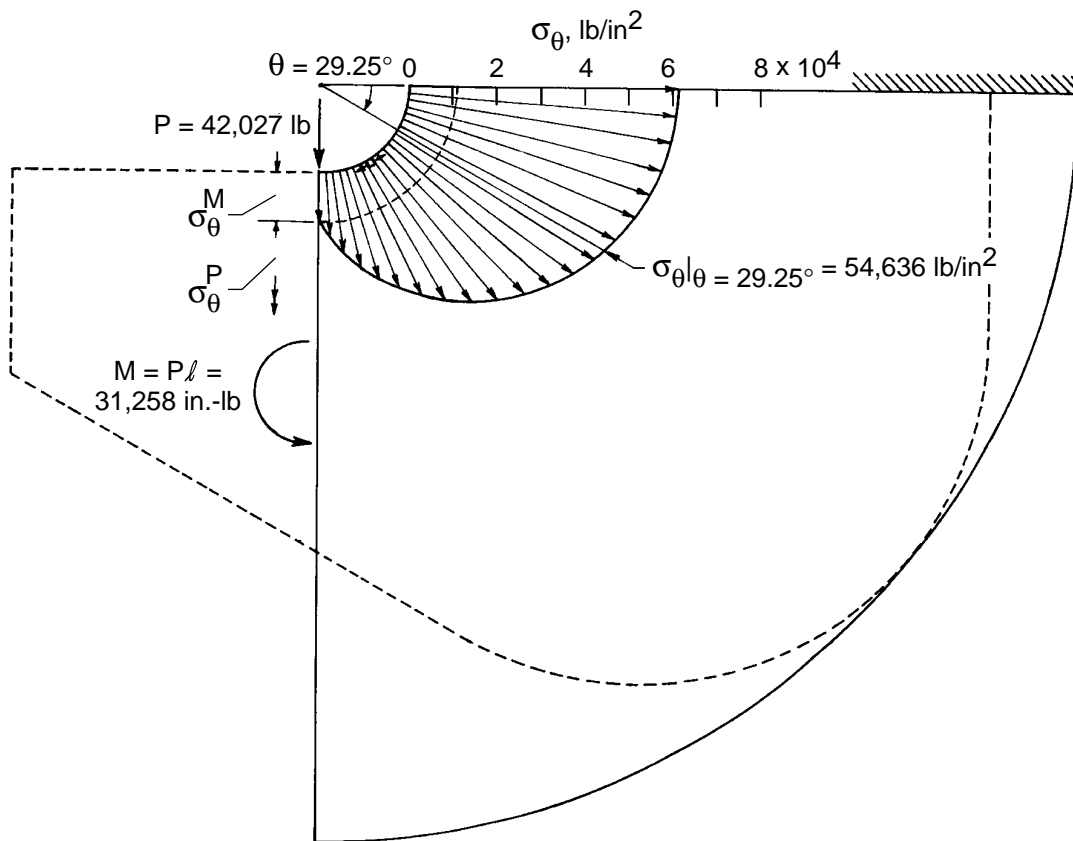
Figure 12. Distributions of tangential stress σ_θ along the inner boundary of the equivalent curved beam; $P = 42{,}027$ lb; $M = 31{,}258$ in-lb.
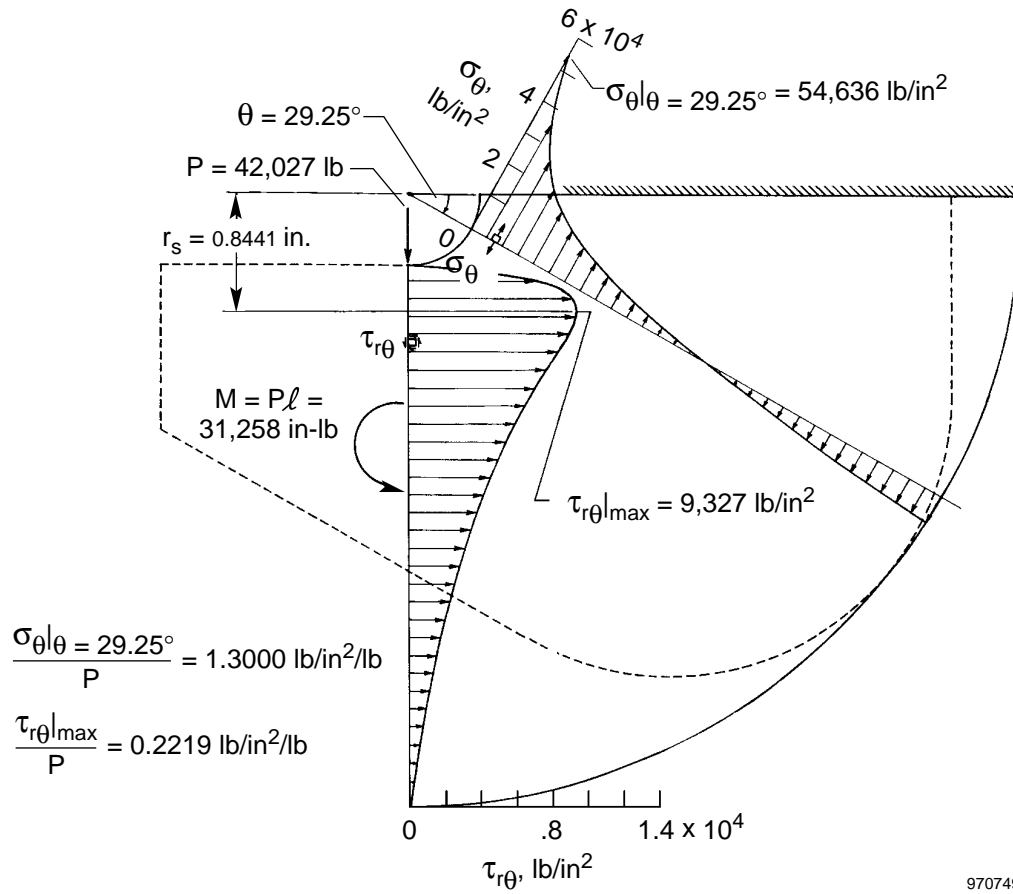
Figure 13. Distributions of tangential stress σ_θ and shear stress $\tau_{r\theta}$ along their respective critical cross section lines; $P = 42{,}027$ lb; $M = 31{,}258$ in-lb.

20

APPENDIX A

Fortran Programs for Equivalent Curved Beam Analysis

```
                            PROGRAM A

c  EQUIVALENT CURVED BEAM THEORY FOR X-38 AND B-5 HOOKS STRESS ANALYSIS
c  1. Tangential stress distribution along equivalent curved beam
c      inner boundary
c  Equivalent curved beam outer boundary circumscribes hook
c      outer boundary
c  Programed by Dr. William L. Ko, March 13, 1997
       PROGRAM B52HOOKS
       DIMENSION SIGP(27)
       DIMENSION TAUP(27)
       DIMENSION SIGT(27)
       DIMENSION SIGM(27)
       DIMENSION PP(27)
       DIMENSION PPP(27)
       DIMENSION SS(27)
       DIMENSION SSS(27)
       DIMENSION XMM(27)
       DIMENSION Y(27)
       DIMENSION X(27)
       REAL X
       DATA X/0.,4.5,9.,11.25,13.5,18.,22.5,26.,26.25,27.,28.75,
      +29.25,31.5,36.,36.25,40.5,45.,49.5,54.,58.5,63.,67.5,72.,
      +76.5,81.,85.5,90./
c  X-38 hook
       A=0.5
       B=4.276880
       e=0.74375
       H=0.01
       P=150.096429
c  B-52 front hook
c      A=0.3125
c      B=1.9
c      e=0.1365
c      h=0.01
c      P=91.4077
c  B-52 old rear hook
c      A=0.16
c      B=1.9
c      e=0.42
c      H=0.01
c      P=185.1242
c  B-52 DAST hook
c      A=0.4375
c      B=2.25
c      e=0.253
```

```
c       H=0.01
c       P=143.2665
c  B-52 new rear hook
c       A=0.5
c       B=2.5
c       e=0.46
c       H=0.01
c       P=156.1775
        C=A/B
        DO 10  I=1,27
        X(I) = X(I)/57.29578
        Y(I) = X(I)*57.29578
        GP=1.-(C**2)+(1.+(C**2))*ALOG(C)
        G=0.25*((1.-C**2)**2)-(C**2)*((ALOG(C))**2)
        SS(I)=COS(X(I))
        SSS(I)=SIN(X(I))
        PP(I)=(P/(B*H*GP))*SS(I)
        PPP(I)=(P/(B*H*GP))*SSS(I)
        XMM(I)=(P*e)/((B**2)*H*G)*(SS(I)/SS(I))
c  Tangential stress at inner boundary due to force P
        SIGP(I)=PP(I)*(3.*(A/B)-(C**2)*((B/A)**3)-(1.+C**2)
      +*(B/A))
c  Tangential stress at inner boundary due to Moment M = Pe
        SIGM(I)=-XMM(I)*(1.-C**2+(C**2)*ALOG(C)*(1.+(B/A)**2)
      +-(1.-C**2)*ALOG(B/A))
c  Shear stress at inner boundary due to force P
        TAUP(I)=-PPP(I)*(A/B+(C**2)*((B/A)**3)-(1.+C**2)*
      +(B/A))
c  Total tangential stress at inner boundary
        SIGT(I)=SIGP(I)+SIGM(I)
        PRINT 100, Y(I), SIGP(I), SIGM(I), SIGT(I), TAUP(I)
100     FORMAT(/1X, F14.5, 4F14.4)
10      CONTINUE
        END
```

22

```
c   EQUIVALENT CURVED BEAM THEORY FOR X-38 HOOK STRESS ANALYSIS
c   1. Distribution of tangential stress along 29.25 degree radial line
c   2. Distribution of shear stress along 90 degree radial line
c   Programed by Dr. William L. Ko, March 13, 1997
      PROGRAM DEPTH
      DIMENSION SIGP(19)
      DIMENSION TAUP(19)
      DIMENSION SIGT(19)
      DIMENSION SIGM(19)
      DIMENSION SIGTH(19)
      DIMENSION R(19)
      REAL B
      DATA R/0.5,.625,.75,.844102,.875,1.,1.25,1.5,1.75,2.,2.25,
     +2.5,2.75,3.,3.25,3.5,3.75,4.,4.14453/
      A=0.5
      B=4.276880
      P=150.096429
      H=0.01
      e=0.74375
      DO 10 I=1,19
      C=A/B
      GP=1.-(C**2)+(1.+(C**2))*ALOG(C)
      G=0.25*((1.-C**2)**2)-(C**2)*((ALOG(C))**2)
      PP=(P/(B*H*GP))
      XMM=(P*e)/((B**2)*H*G)
c   Tangential stress on 0 degree radial line due to force P
      SIGP(I)=PP*(3.*(R(I)/B)-(C**2)*((B/R(I))**3)-(1.+C**2)
     +*(B/R(I)))
c   Tangential stress due to Moment M = Pe
      SIGM(I)=-XMM*(1.-C**2+(C**2)*ALOG(C)*(1.+(B/R(I))**2)
     +-(1.-C**2)*ALOG(B/R(I)))
c   Shear stress on 90 degree radial line due to force P
      TAUP(I)=-PP*(R(I)/B+(C**2)*((B/R(I))**3)-(1.+C**2)*
     +(B/R(I)))
c   Tangential stress on 29.25 degree radial line due to force P
c   Cos(29.25 degree) = 0.872496
      SIGTH(I)=SIGP(I)*(0.872496)
c   Total tangential stress along 29.25 degree radial line
      SIGT(I)=SIGTH(I)+SIGM(I)
      PRINT 100, R(I), SIGTH(I), SIGM(I), SIGT(I), TAUP(I)
100   FORMAT(/1X, F12.5, 4F12.4)
10    CONTINUE
      END
```
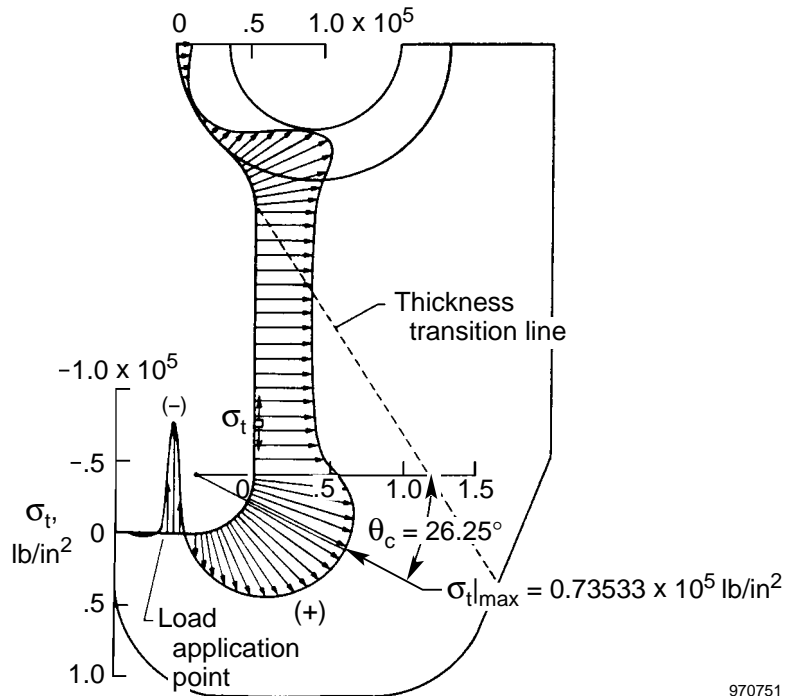
APPENDIX B

Stress Distributions in B-52 Original Pylon Hooks
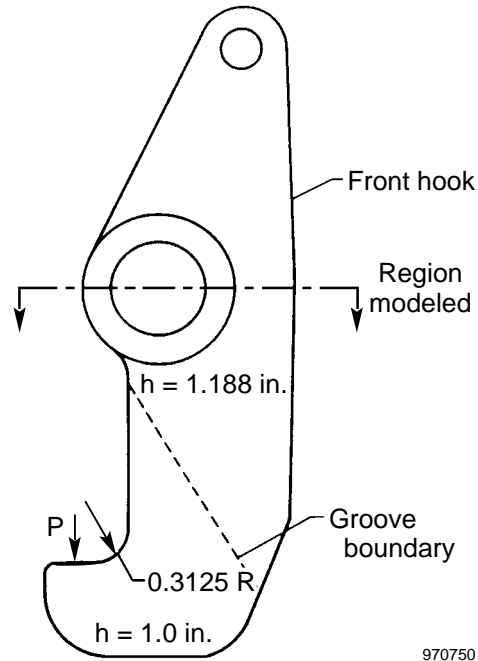
Figure B-1. Geometry of the B-52 original pylon front hook.

Figure B-2. Distribution of tangential stress σ_t along inner boundary of the front hook; $P = 10,000$ lb.
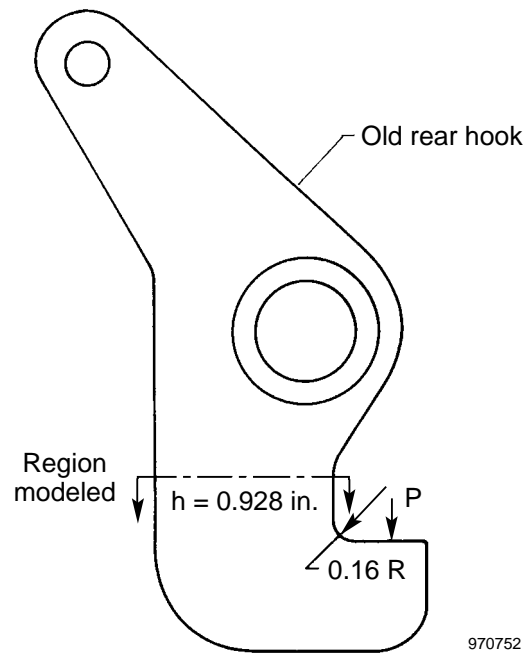
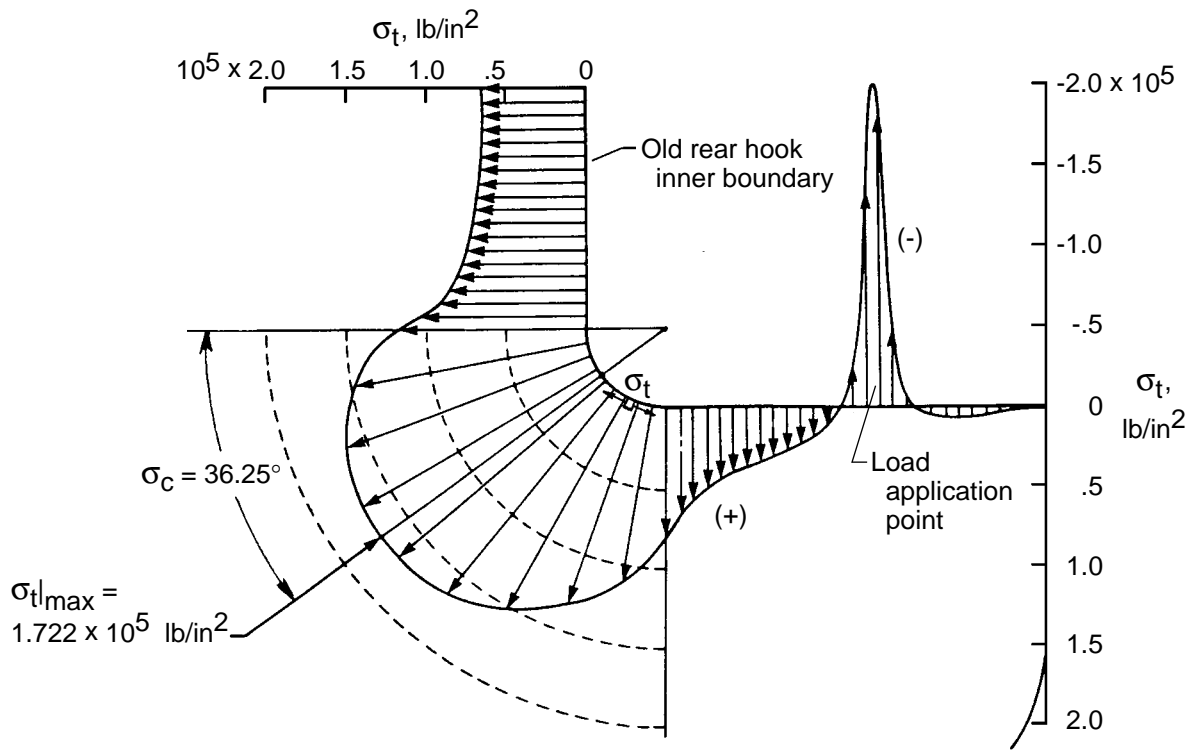Figure B-3. Geometry of the B-52 original pylon old rear hook.

Figure B-4. Distribution of tangential stress σ_t along inner boundary of old the rear hook; $P = 17{,}179.53$ lb.
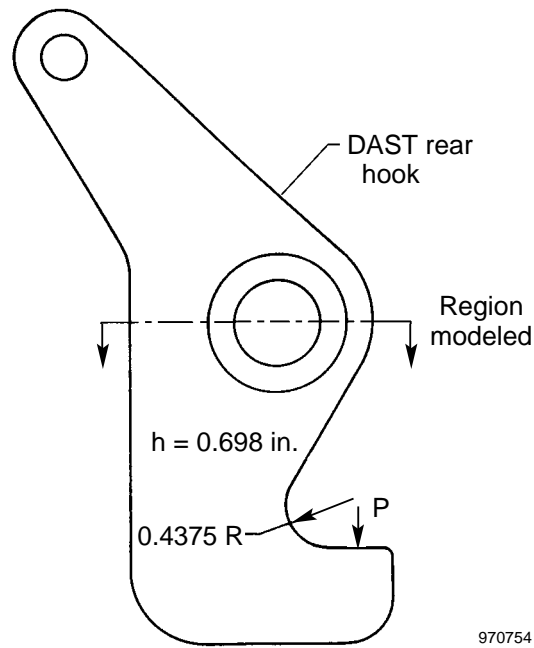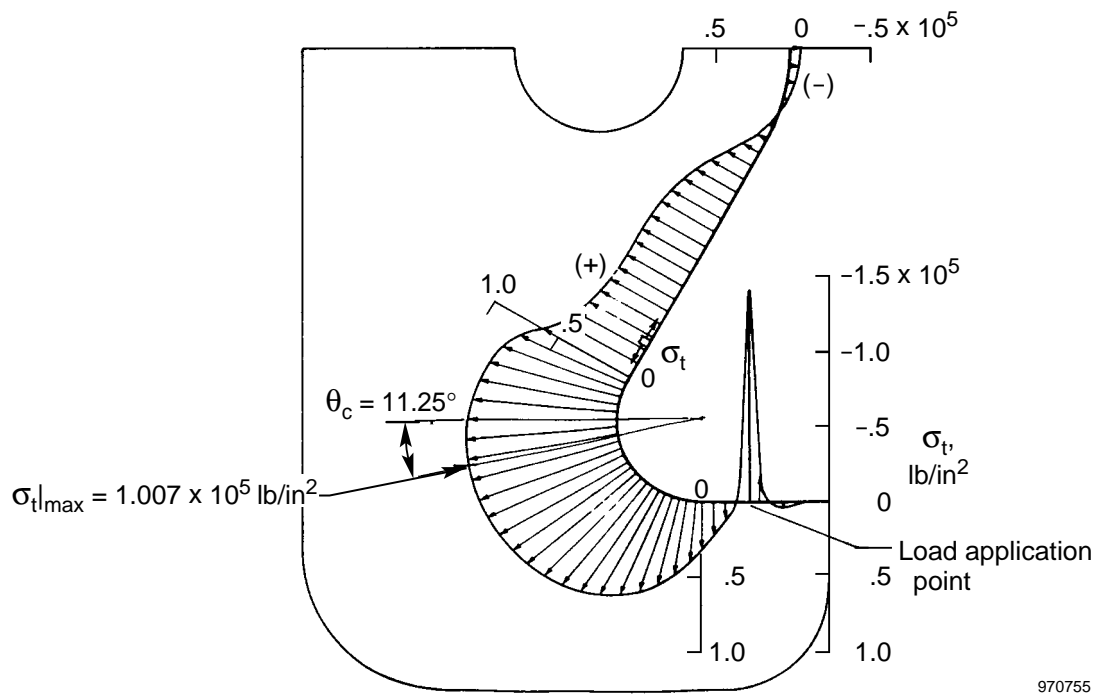
Figure B-5. Geometry of the B-52 original pylon DAST rear hook.

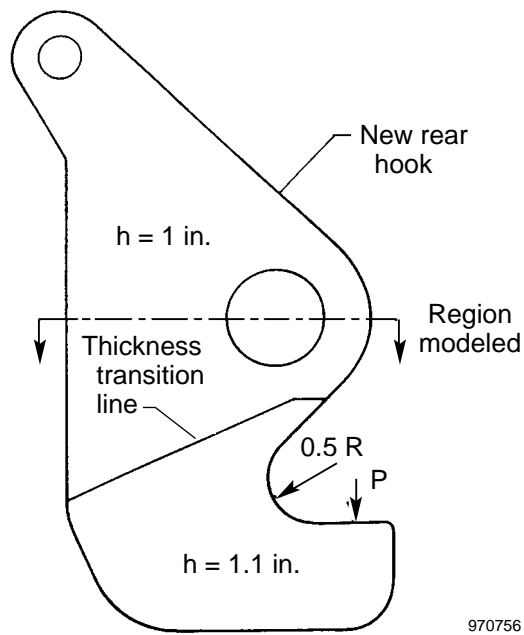Figure B-6. Distribution of tangential stress σ_t along inner boundary of the DAST rear hook; $P = 10,000$ lb.
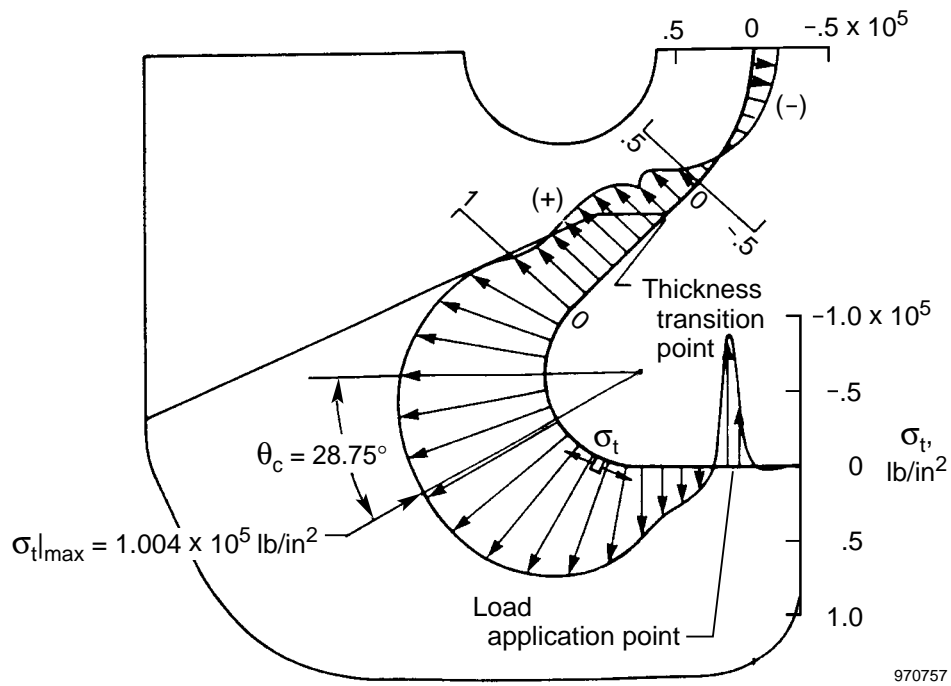
Figure B-7. Geometry of the B-52 original pylon new rear hook.

Figure B-8. Distribution of tangential stress σ_t along inner boundary of the new rear hook; $P = 17{,}179.53$ lb.

REFERENCES

1. Whetstone, W. D., *SPAR Structural Analysis System Reference Manual, System Level 13A, Vol. 1, Program Execution*, NASA CR-158970-1, Dec. 1978.

2. Ko, William L., *Delamination Stresses in Semicircular Laminated Composite Bars*, NASA TM-4026, Jan. 1988.

3. Ko, William L. and Raymond H. Jackson, *Multilayer Theory for Delamination Analysis of a Composite Curved Bar Subjected to End Forces and End Moments*, NASA TM-4139, Sept. 1989. Also published in *Composite Structures 5*, I. H. Marshall, ed., Elsevier Applied Science, London, 1989, pp. 173–198.

4. Ko, William L. and Raymond H. Jackson, *Open-Mode Delamination Stress Concentrations in Horseshoe and Elliptic Composite Curved Bars Subjected to End Forces*, NASA TM-4164, Jan. 1990.

5. Lekhnitskii, S. G., *Anisotropic Plates*, Gordon and Breach Science Publishers, New York, 1968.

6. Ko, William L., *Stress Analyses of B-52 Pylon Hooks*, NASA TM-84924, Oct. 1985.

REPORT DOCUMENTATION PAGE

1. AGENCY USE ONLY (Leave blank)	2. REPORT DATE October 1997	3. REPORT TYPE AND DATES COVERED Technical Memorandum

4. TITLE AND SUBTITLE

Stress Analysis of B-52 Pylon Hooks for Carrying the X-38 Drop Test Vehicle

6. AUTHOR(S)

William L. Ko

5. FUNDING NUMBERS

WU 250 88 00

7. PERFORMING ORGANIZATION NAME(S) AND ADDRESS(ES)

NASA Dryden Flight Research Center
P.O. Box 273
Edwards, California 93523-0273

8. PERFORMING ORGANIZATION REPORT NUMBER

H-2187

9. SPONSORING/MONITORING AGENCY NAME(S) AND ADDRESS(ES)

National Aeronautics and Space Administration
Washington, DC 20546-0001

10. SPONSORING/MONITORING AGENCY REPORT NUMBER

NASA/TM-97-206218

11. SUPPLEMENTARY NOTES

12a. DISTRIBUTION/AVAILABILITY STATEMENT

Unclassified—Unlimited
Subject Category 39

12b. DISTRIBUTION CODE

13. ABSTRACT (Maximum 200 words)

The finite-element structural analysis method was used in a two-dimensional stress concentration analysis of a new pylon hook for carrying the X-38 lifting body atmospheric drop test vehicle on the B-52 carrier aircraft. The stress distributions in the hook were obtained, and the critical stress points were identified. The functional relationships between the applied hook load and the induced maximum tangential and shear stresses were established for setting the limit hook load for test flights. By properly representing the X-38 hook with an equivalent curved beam, the conventional curved beam theory predicted the values of the maximum tangential and shear stresses quite close to those calculated from the finite-element analysis. The equivalent curved beam method may be of practical value during the initial stage of the hook design in estimating the critical stresses and failure loads with reasonable accuracy.

14. SUBJECT TERMS

Equivalent curved beam theory, Finite element stress analysis , Stress concentrations, X-38 hooks

15. NUMBER OF PAGES
34

16. PRICE CODE
A03

17. SECURITY CLASSIFICATION OF REPORT	18. SECURITY CLASSIFICATION OF THIS PAGE	19. SECURITY CLASSIFICATION OF ABSTRACT	20. LIMITATION OF ABSTRACT
Unclassified	Unclassified	Unclassified	Unlimited